NASA Technical Memorandum 100863

Fatigue Crack Growth Behavior of a Single Crystal Alloy as Observed Through an In Situ Fatigue Loading Stage

Jack Telesman and Peter Kantzos
Lewis Research Center
Cleveland, Ohio

Prepared for the
SAMPE Metals Processing Conference
Dayton, Ohio, August 2–4, 1988

NASA

FATIGUE CRACK GROWTH BEHAVIOR OF A SINGLE CRYSTAL ALLOY AS OBSERVED THROUGH AN IN SITU FATIGUE LOADING STAGE

Jack Telesman and Peter Kantzos*
National Aeronautics and Space Administration
Lewis Research Center
Cleveland, Ohio 44135

Abstract

An in situ fatigue loading stage inside a scanning electron microscope (SEM) was used to determine the fatigue crack growth behavior of a PWA 1480 single-crystal nickel-based superalloy. The loading stage permits real-time viewing of the fatigue damage processes at high magnifications.

The PWA 1480 single-crystal, single-edge notch specimens were tested with the load axis parallel to the (100) orientation. Two distinct fatigue failure mechanisms were identified. The crack growth rate differed substantially when the failure occurred on a single slip system in comparison to multi-slip system failure. Two processes by which crack branching is produced were identified and are discussed. Also discussed are the observed crack closure mechanisms.

I. INTRODUCTION

Single-crystal nickel-based superalloys are being utilized in advanced turbine engine applications and are also candidate materials for the use in space shuttle main engines. Due to the current emphasis on the damage tolerant design for turbine engine components, the understanding of fatigue crack growth (FCG) behavior of these alloys has become increasingly more important.

Single-crystal alloys have also been used for fundamental studies of the fatigue damage mechanisms. These alloys are ideal candidates for such studies since they eliminate number of problems encountered with polycrystalline alloys. In polycrystalline alloys, the fatigue crack front encompasses many grains of various unknown orientations, with each grain individually contributing to the overall FCG behavior. The measured fatigue crack growth rate is an average of these contributions and is also effected by the interaction of the crack front with a myriad of grain boundaries. These problems are not encountered when the fatigue behavior of the single-crystal alloys are studied.

In order to obtain a better understanding of the fatigue damage mechanisms, a fatigue loading stage inside a scanning electron microscope (SEM) was developed at NASA Lewis. The small loading stage consists of a specially designed closed loop, servohydraulic load frame mounted inside a SEM. This unique device permits real-time

*NASA Resident Research Associate.

viewing of the fatigue damage processes at high magnifications. An attached video tape recorder and monitor allow repeated test viewing for a more detailed evaluation of the pertinent fatigue mechanisms. The loading stage is detailed elsewhere,[1] however a summary of the operational characteristics is shown in Table 1.

The fatigue loading stage was used to determine the fatigue crack growth damage mechanisms of PWA 1480, a single-crystal nickel-based superalloy.

2. EXPERIMENTAL PROCEDURE

Cast billets of the PWA 1480 single-crystal alloy were obtained in a near (100) orientation. The nominal composition of the alloy is shown in Table 2. Single-edge notched (SEN) specimens of the geometry shown in Fig. 1 were machined using electrical discharge machining. The faces of the SEN specimens were nearly parallel to the (001) orientation. Prior to testing, the specimen faces were polished through a 1-μm diamond paste. Two of the four specimens were then etched to reveal the precipitate structure. Testing was performed in the loading stage. Three of the four specimens were tested at a load ratio R (minimum load/maximum load) of 0.1 with the maximum load being 3110 N (700 lb). The other specimen was tested at R = 0.5 with the maximum load being 2220 N (500 lb). The testing was conducted at room temperature at a frequency of 10 Hz. The vacuum inside the SEM ranged from 1x10-7 to 5x10-7 torr. Tests were stopped periodically to obtain high magnification micrographs of the crack front. Crack growth measurements were obtained for the R = 0.5 specimen and one of the R = 0.1 specimens, while the other two specimens were used to make general observations of the fatigue processes. In all cases the crack length was taken to be the projection of the crack on to a plane perpendicular to the loading axis. To ease the determination of the crack tip location, the micrographs were obtained typically at the maximum load. The crack tip was taken to be the furthest point where displacement between the two surfaces was observed. Some post failure fractography was also performed.

3. RESULTS AND DISCUSSION

3.1 Crack Propagation Mechanisms

The surface observations revealed two distinctive fatigue failure mechanisms. When viewed at low magnifications, the crack growth was either in the plane perpendicular to the loading direction ("straight" crack shown in Fig. 2(a)), or at an inclined angle to the loading axis (Fig. 2(b)). Interestingly, both modes of crack growth were sometimes encountered in the same specimen. For instance, on one side of specimen SC6 tested at R = 0.5, the crack grew perpendicular to the loading direction, while on the other side an inclined crack of approximately 60° to the loading axis was present.

Higher magnification views of the "straight" crack reveal that in reality the crack for the most part propagated on two competing, distinct slip systems. This process has also been observed by Neumann[2] in a copper single crystal. The process consists of alternating shear decohesion at the crack tip on two intersecting (111) type planes creating an "unzipping" effect.[3] This failure mechanism results in activation of large number of slip planes at the crack tip as shown in Fig. 3. As a result, a large deformation zone was formed in the crack wake.

The process through which the fatigue crack growth on an inclined plane occurs is somewhat different. In this case only one (111) type slip system was activated and the crack tended to follow it as shown in Figs. 4(a) and 4(b). Very few slip planes were activated ahead of the crack tip, thus the damage zone was very small. The actual crack growth mechanism appears to be a combination of slip damage on the active

(111) plane due to the resolved shear stresses, combined with the tensile stresses normal to this plane which separate the surfaces on each side of the slipped and damaged material. When this type of mechanism is operative, it becomes difficult to locate precisely the location of the crack tip due to the indistinguishability between the areas where only slip damage has occurred versus areas where the separation of the surfaces has taken place (Figs. 4(a) and 4(b)). At times, the crack-advancement mechanism also involved linking of cracks on parallel slip bands, as shown in Fig. 5, and also documented by Wu and Hoeppner.[4]

The surface observations revealed that the failure mechanisms were mostly confined to the damage on the (111) type slip planes in agreement with findings of others[5,6] for nickel-based single crystals tested at room temperature. However, a post failure analysis revealed the presence of another failure mechanism. A fracture surface of one of the failed specimens was etched and analyzed under the SEM. The evaluation revealed the presence of cuboidal facets of the strengthening precipitates on the fracture surface which is indicative of (100) type failure (Fig. 6(a)). These regions of probable (100) failure were present only in the mid-thickness of the specimen tested under relatively low stress intensities. As the stress intensity increased, the failure mechanism changed in the mid-thickness to the (111) type as indicated by the presence of the (111) facets (Fig. 6(b)).

3.2 Effect of Failure Mode on FCG Rate

The crack length versus cycles plots of specimens tested at a R ratio of 0.1 and 0.5 are shown respectively in Figs. 7(a) and 7(b). Specimen SC2, tested at R = 0.1, exhibited macroscopic crack growth perpendicular to the loading axis on both sides of the specimen. The FCG behavior on each side of this specimen was similar. Specimen SC6 tested at R = 0.5 exhibited macroscopically "straight" crack growth on one side and an inclined crack growth on the other side. At first, crack growth was only observed on the side exhibiting inclined growth (Fig. 7(b), Side A). However, once the "straight" crack appeared on the other surface, it quickly began growing more rapidly than its counterpart on Side A (Fig. 7(b), Side B). FCG rates were calculated on each side of this specimen as a function of the crack length and are shown in Fig. 8. The FCG rates on the side which exhibited "straight" crack growth and deformation on the multislip systems, are faster than the crack growth rates observed on the other side where the crack growth was at an inclined angle and the damaging slip was mostly limited to one slip system. These results imply that damage mechanisms can have a significant effect on FCG behavior. However, since only surface observations and measurements were performed, it is not clear how the subsurface interaction between the two active failure mechanisms influences the observed surface FCG behavior. More work is required to fully comprehend the role of these failure mechanisms on FCG behavior. Ideally, a direct comparison of behavior of a specimen exhibiting entirely inclined crack growth with one exhibiting only "straight" crack growth is desired.

3.3 Mechanisms of Crack Branching and Crack Closure

The observed mechanisms of crack branching can be divided into two categories. One category consisted of a secondary crack developing at or slightly behind the crack tip as shown in Fig. 9. These cracks were usually formed on the slip bands. The usual sequence of events consisted of slowing down of the crack growth rate of the main crack, followed by the initiation of another crack slightly behind the crack tip on the other competing slip system. The new crack then started growing rapidly, leaving in its wake the

original crack tip which became in effect the branched crack segment.

The other type of crack branching mechanism encountered consisted of a crack nucleating ahead of the main crack, followed by the coalescence of the two cracks slightly behind the original crack tip. This sequence of events is illustrated in Fig. 10. As shown, crack nucleation was preceded by formation of a slip band (Fig. 10(a) and 10(b)), followed by an initiation of another crack ahead of the crack tip on a parallel slip band (Fig. 10(c)), and finally the coalescence of the three cracks (Fig. 10(d)). Post failure evaluations of some of the events described above, revealed that the surface observations can at times be misleading. What may appear on the surface to be the initiation of an entirely new crack, may in fact be the surfacing of a branched, subsurfaced, region of the main crack.

Three different mechanisms of crack closure were observed to occur in this nickel-based superalloy single crystal. Due to the high degree of tortuosity of the crack path, interlocking of asperities occurred in the crack wake as demonstrated in Fig. 11(a) (roughness induced closure). Another method by which crack closure was found to occur was through the lodging of debris, formed during the fatigue processes, between the two cracked surfaces (Fig. 11(b)). Crack closure was also found to depend upon the mode of loading in the crack segments near the crack tip. This was probably the most common and important mechanism of crack closure. Segments of the crack which experienced mostly Mode I loading (tensile type), exhibited the largest crack tip opening displacements (CTOD) and tended to remain open throughout most of the loading cycle. Other segments, subjected to mixed-mode loading (combination of tensile and shear), exhibited much smaller CTOD and were closed for considerably longer portions of the loading cycle. This behavior is clearly shown in Figs. 11(c) and 11(d). The larger magnitude of crack closure of the inclined crack subjected to mixed mode loading, may have contributed to its lower observed FCG rates since the crack tip was closed for longer portions of the loading cycle.

4. SUMMARY

The in situ fatigue loading stage inside a SEM has proven to be a powerful tool in identifying the fatigue failure mechanisms. Using this tool, relationships between the measured FCG rates and the individual fatigue failure mechanisms were established for the PWA 1480 single-crystal nickel-based superalloy. The crack growth rate was substantially lower when the failure occurred on a single (111) slip system in comparison to the multislip failure. The details of two different processes resulting in formation of crack branching were observed. Three different crack closure mechanisms were identified.

The in situ loading stage is capable of providing qualitative information such as the mode of failure, as well as quantitative information such as CTOD and the magnitude of crack closure load. Such information is needed to improve the fundamental understanding of the fatigue damage processes as well as life prediction methodology of engineering structures.

5. REFERENCES

1. J. Telesman, P. Kantzos, and D.M. Fisher, "Fatigue Loading Stage Combined with Scanning Electron Microscope," NASA TM-100822, 1988.

2. P. Neumann, "New Experiments Concerning the Slip Processes at Propagating Fatigue Cracks - I," Acta Met., Vol. 22, No. 9, Sept. 1974, pp. 1155-1178.

3. C.Y. Yang, and H.W. Liu, "The Application of the Unzipping Model of Fatigue Crack Growth to Micro-Cracks," Scr. Met., Vol. 14, No. 7, July 1980, pp. 785-790.

4. D.C. Wu, and D.W. Hoeppner, "Observations and Characterization Considerations of Fatigue Crack Growth in a Single Crystal Nickel-Base Superalloy," Scr. Met., Vol. 19, No. 4, Apr. 1985, pp. 493-498.

5. J.S. Crompton, and J.W. Martin, "Crack Growth in a Single Crystal Superalloy at Elevated Temperatures," Metall. Trans. A., Vol. 15, No. 9, Sept. 1984, pp. 1711-1719.

6. C. Howland, and C.W. Brown, "The Effect of Orientation on Fatigue Crack Growth in a Nickel-Based Single-Crystal Superalloy," Report No. PNR-90207, Rolls Royce Ltd., Derby, England, 1984.

TABLE I. - SEM LOADING STAGE CHARACTERISTICS

Maximum cyclic load, N (lb)	4450 (1000)
Maximum cyclic frequency, Hz	30
Maximum temperature (designed), °C (°F)	1100 (2000)
Working distance (room temp. stage), mm (in.)	25 (1)
Working distance (high temp. stage), mm (in.)	55 (2.2)
Useful maximum magnification (room temp. stage)	10 000X
Useful maximum magnification (high temp. stage)	3000X

TABLE 2. - PWA 1480

NOMINAL COMPOSITION

Element	Weight percent
Co	5
Cr	10
W	4
Ta	12
Al	5
Ti	1.5
Ni	62

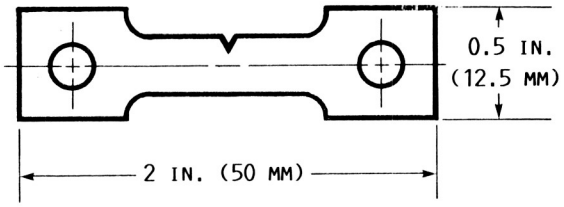

FIGURE 1. - SINGLE-EDGE NOTCH SPECIMEN.

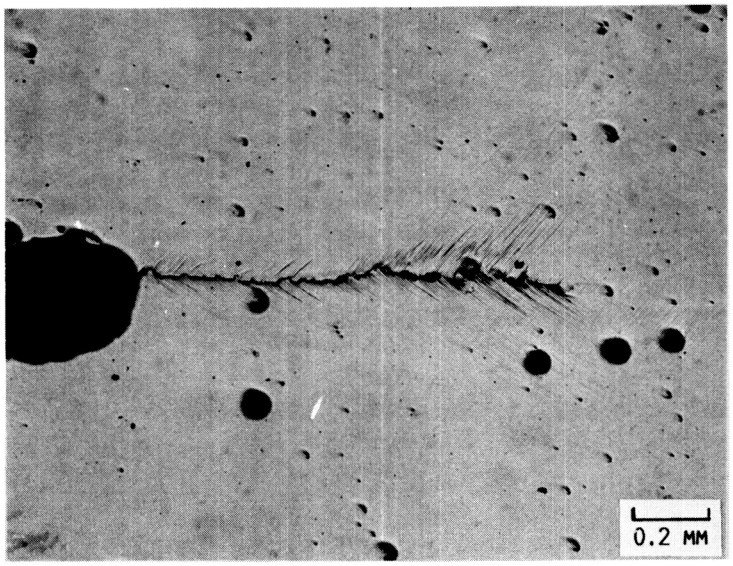

(a) NORMAL TO THE LOADING DIRECTION.

LOADING
AXIS

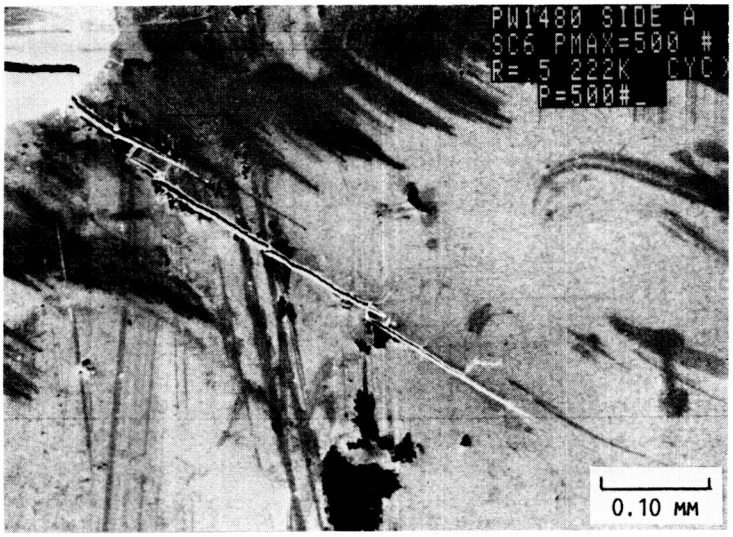

(b) INCLINED TO THE LOADING DIRECTION.

FIGURE 2. - CRACK PROPAGATION DIRECTIONS IN PWA 1480.

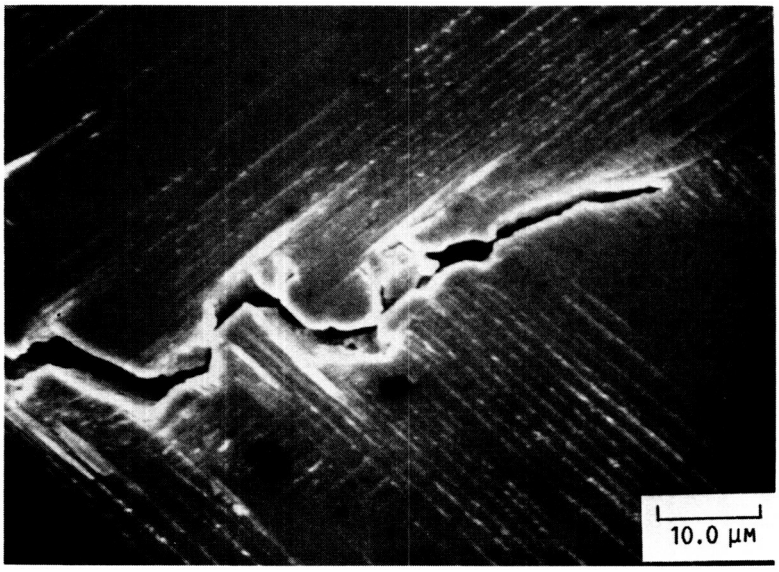

FIGURE 3. - HIGH MAGNIFICATION OF THE MACROSCOPICALLY STRAIGHT CRACK. TWO SLIP SYSTEMS AND A LARGE NUMBER OF SLIP PLANES WERE ACTIVATED.

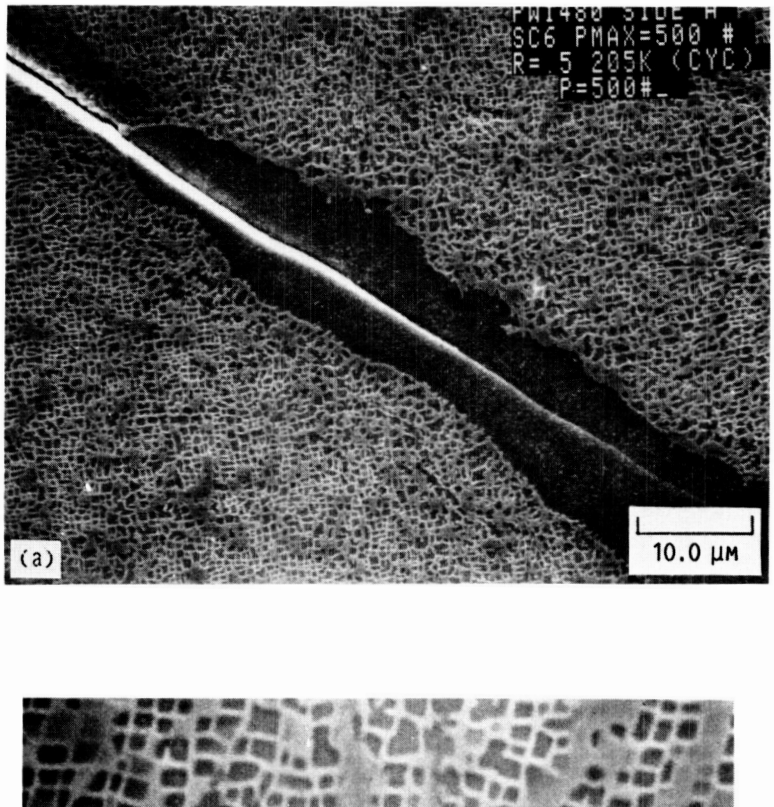

FIGURE 4. - GROWTH OF AN INCLINED CRACK, PARALLEL TO ONE SLIP SYSTEM. VERY FEW SLIP PLANES WERE ACTIVATED AND SLIP WAS RESTRICTED PRIMARILY TO ONE (111) SLIP SYSTEM.

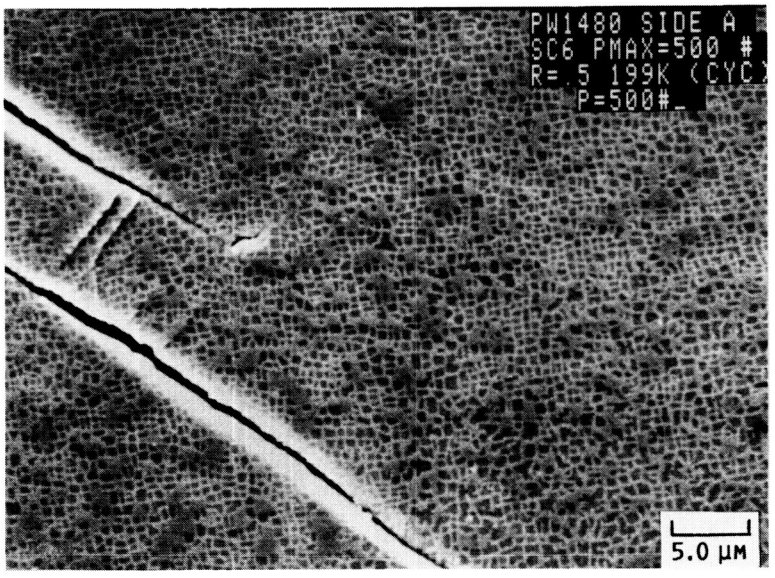

FIGURE 5. - LINKING OF TWO SEGMENTS OF AN INCLINED CRACK.

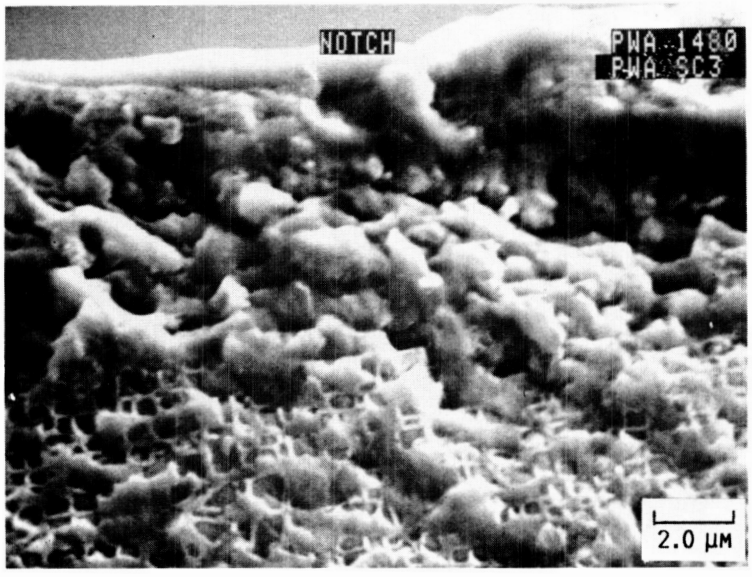

(a) LOW ΔK REVEALED AREAS OF (100) FAILURE.

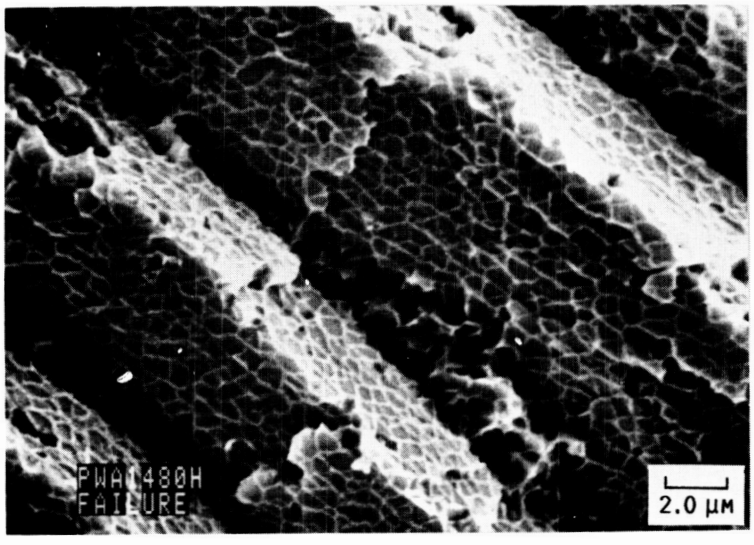

(b) HIGH ΔK REVEALED STRICTLY (111) FAILURE.

FIGURE 6. - MID-THICKNESS FRACTURE SURFACES.

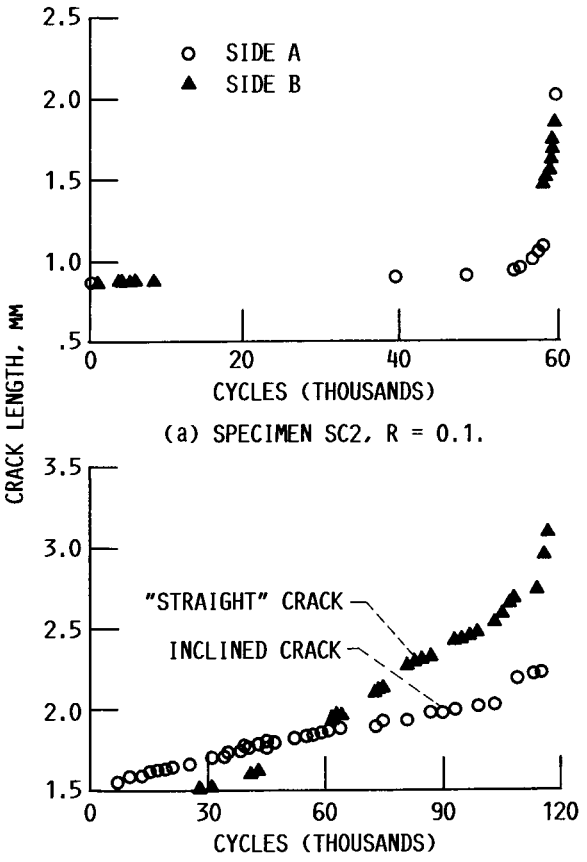

(a) SPECIMEN SC2, R = 0.1.

(b) SPECIMEN SC6, R = 0.5.

FIGURE 7. - CRACK LENGTH VERSUS CYCLES FOR TWO PWA 1480 SPECIMENS.

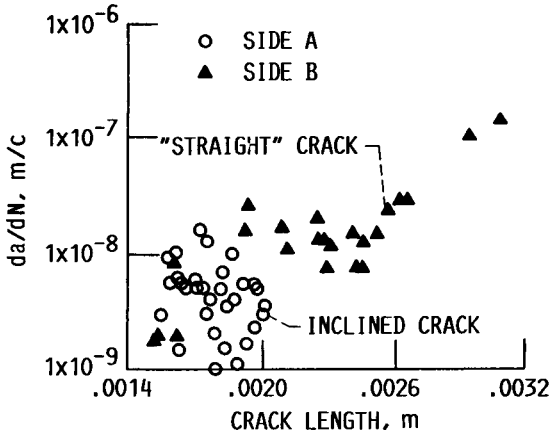

FIGURE 8. - CRACK GROWTH RATE VERSUS CRACK LENGTH FOR SPECIMEN SC6 WHICH EXHIBITED TWO TYPES OF CRACKING PROCESSES.

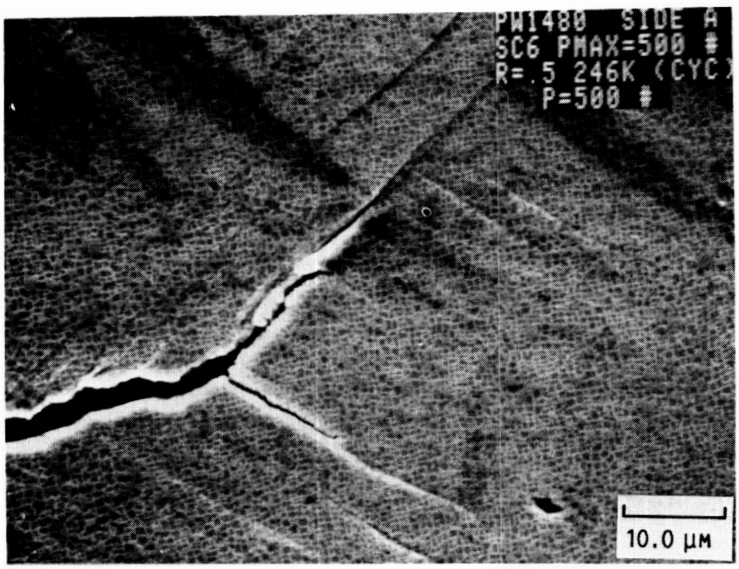

FIGURE 9. - CRACK BRANCHING NEAR THE CRACK TIP (MAXIMUM LOAD).

(a) 186 000 CYCLES.

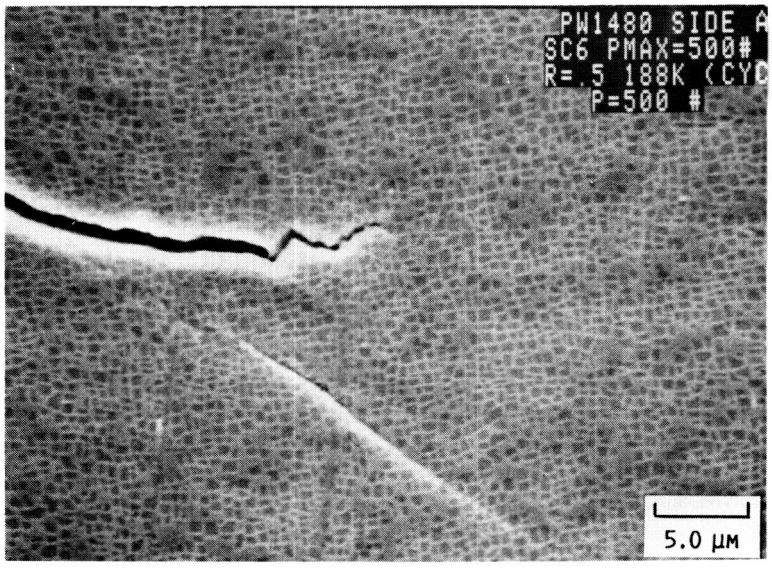

LOADING AXIS

(b) 188 000 CYCLES.

FIGURE 10. - THE SEQUENCE OF CRACK INITIATION AND LINKUP OF SLIP BAND CRACKS WITH THE MAIN CRACK (MICROGRAPHS TAKEN AT MAXIMUM LOAD).

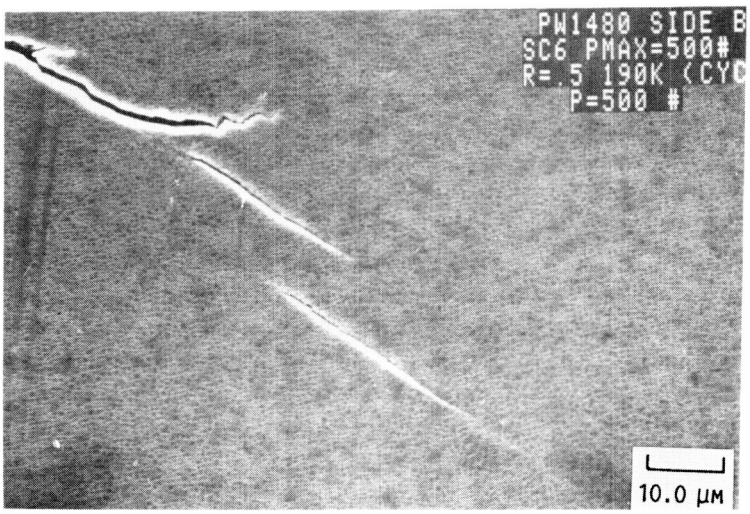

(c) 190 000 CYCLES.

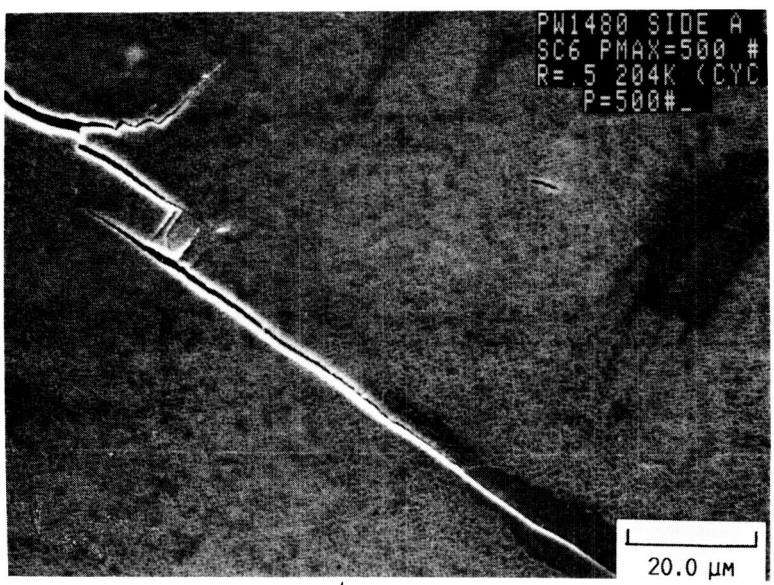

LOADING AXIS

(d) 204 000 CYCLES.

FIGURE 10. - CONCLUDED.

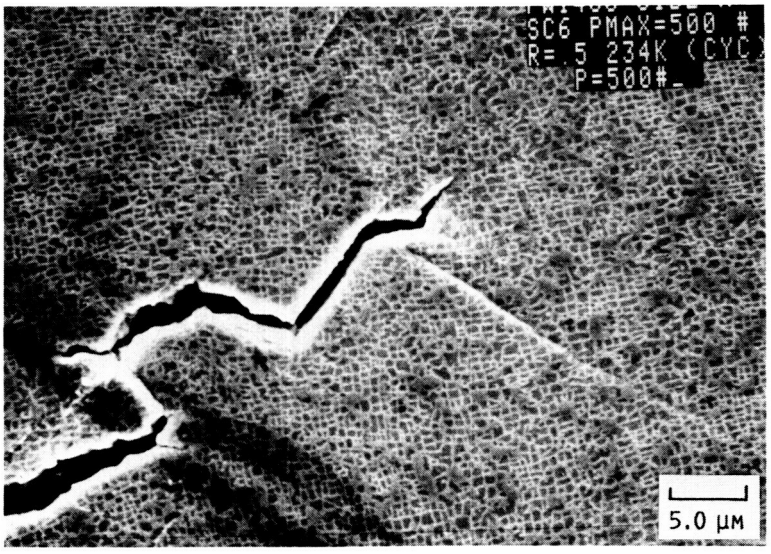

(a) 2220 N (500 LB).

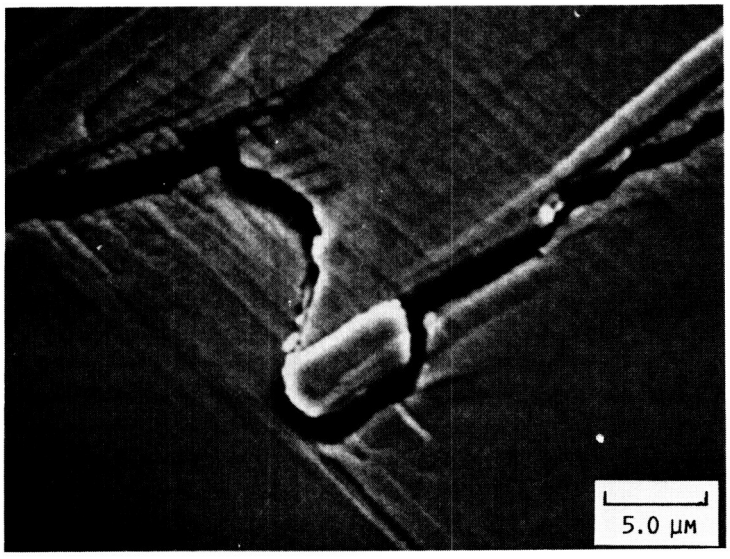

(b) 2220 N (500 LB).

LOADING AXIS

FIGURE 11. - THREE MECHANISMS OF CRACK CLOSURE ARE: ROUGHNESS INDUCED (a), DEBRIS FORMATION (b), AND THE EFFECT OF MIXED MODE LOADING (c) AND (d).

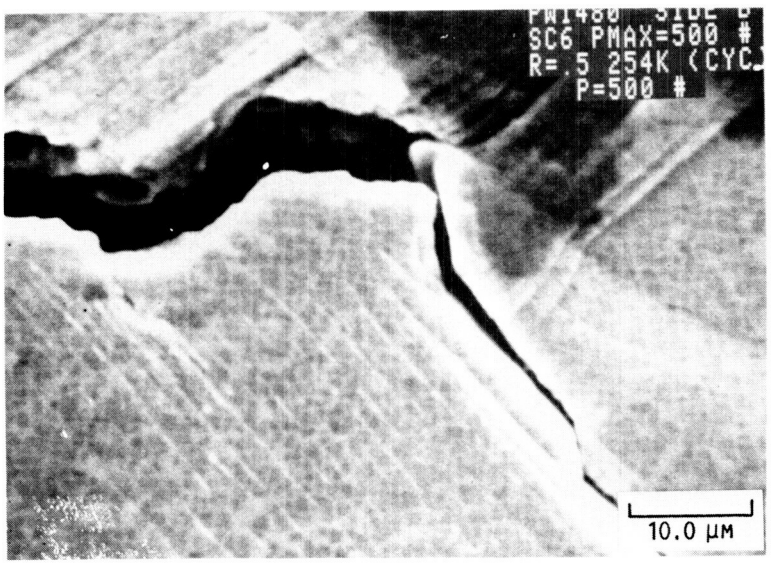

(c) 2220 N (500 LB).

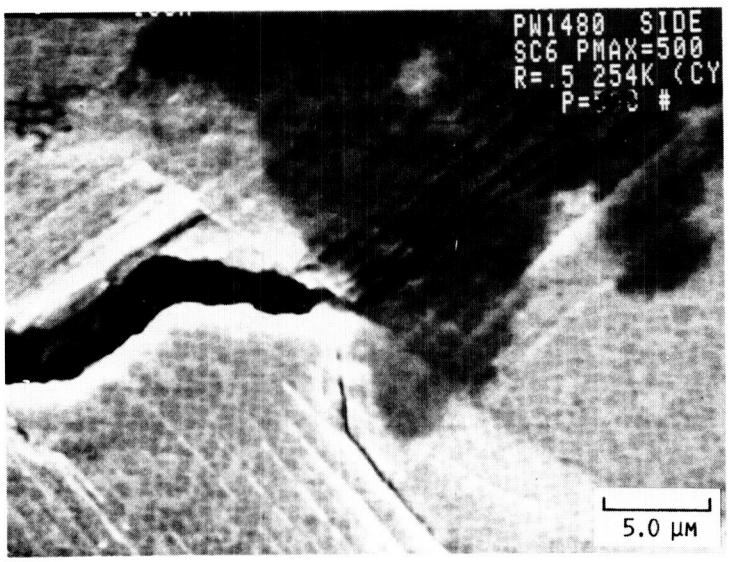

(d) 1335 N (300 LB).

LOADING AXIS

FIGURE 11. - CONCLUDED.

NASA
National Aeronautics and Space Administration

Report Documentation Page

1. Report No.	2. Government Accession No.	3. Recipient's Catalog No.
NASA TM-100863		

4. Title and Subtitle

Fatigue Crack Growth Behavior of a Single Crystal Alloy as Observed Through an In Situ Fatigue Loading Stage

5. Report Date

6. Performing Organization Code

7. Author(s)

Jack Telesman and Peter Kantzos

8. Performing Organization Report No.

E-4080

10. Work Unit No.

505-63-1B

9. Performing Organization Name and Address

National Aeronautics and Space Administration
Lewis Research Center
Cleveland, Ohio 44135-3191

11. Contract or Grant No.

13. Type of Report and Period Covered

Technical Memorandum

12. Sponsoring Agency Name and Address

National Aeronautics and Space Administration
Washington, D.C. 20546-0001

14. Sponsoring Agency Code

15. Supplementary Notes

Prepared for the SAMPE Metals Processing Conference, Dayton, Ohio, August 2-4, 1988. Jack Telesman, NASA Lewis Research Center; Peter Kantzos, NASA Resident Research Associate.

16. Abstract

An in situ fatigue loading stage inside a scanning electron microscope (SEM) was used to determine the fatigue crack growth behavior of a PWA 1480 single-crystal nickel-based superalloy. The loading stage permits real-time viewing of the fatigue damage processes at high magnifications. The PWA 1480 single-crystal, single-edge notch specimens were tested with the load axis parallel to the (100) orientation. Two distinct fatigue failure mechanisms were identified. The crack growth rate differed substantially when the failure occurred on a single slip system in comparison to multislip system failure. Two processes by which crack branching is produced were identified and are discussed. Also discussed are the observed crack closure mechanisms.

17. Key Words (Suggested by Author(s))	18. Distribution Statement
Single crystal Fatigue crack growth Fatigue loading stage Superalloys	Unclassified - Unlimited Subject Category 26

19. Security Classif. (of this report)	20. Security Classif. (of this page)	21. No of pages	22. Price*
Unclassified	Unclassified	18	A02

NASA FORM 1626 OCT 86

*For sale by the National Technical Information Service, Springfield, Virginia 22161